Exploring the Conformational Space of Growth Hormone-Releasing Hormone Analogs using Dopant Assisted Trapped Ion Mobility Spectrometry – Mass Spectrometry

Kevin Jeanne Dit Fouque,[†] Javier Moreno[†] and Francisco Fernandez-Lima *,[†,§]

[†] Department of Chemistry and Biochemistry, Florida International University, 11200 SW 8th St., AHC4-233, Miami, FL 33199, United States.

[§] Biomolecular Sciences Institute, Florida International University, 11200 SW 8th St., AHC4-211, Miami, FL 33199, United States.

ABSTRACT: Recently, we proposed a high-throughput screening workflow for the elucidation of agonistic or antagonistic growth hormone – releasing hormone (GHRH) potencies based on structural motif descriptors as a function of the starting solution. In the present work, we revisited the influence of solution and gas-phase GHRH molecular micro-environment using trapped ion mobility – mass spectrometry (TIMS-MS). The effect of the starting solvent composition (10 mM ammonium acetate (NH4Ac), 50% methanol (MeOH), 50% acetonitrile (MeCN) and 50% acetone (Ac)) and gas-phase modifiers (N_2, N_2+MeOH, N_2+MeCN and N_2+Ac) on the conformational states of three GHRH analogs, GHRH (1-29), MR-406 and MIA-602 is described as a function of the trapping time (100 – 500 ms). Changes in the mobility profiles were observed showing the dependence of the conformational states of GHRH analogs according to the molecular micro-environment in solution, suggesting the presence of solution memory effects on the gas-phase observed structures. Modifying the bath gas composition resulted in smaller mobilities that are correlated with the size and mass of the organic modifier, and more importantly led to substantial changes in relative abundances of the IMS profiles. We attributed the observed changes in the mobility profiles by a clustering/de-clustering mechanism between the GHRH analog ions and the gas modifiers, re-defining the free energy landscape and leading to other local minima structures. Moreover, inspection of the mobility profiles as a function of the trapping time (100 to 500 ms) allowed for conformational inter-conversions toward more stable "gas-phase" structures. These experiments enabled us to outline a more detailed description of the structures and intermediates involved in the biological activity of GHRH, MR-406 and MIA-602.

1. INTRODUCTION

Ion mobility spectrometry – mass spectrometry (IMS-MS) has demonstrated significant advances for the investigation of the conformational states that adopt biomolecules by varying the molecular micro-environment, including biologically-relevant conditions.[1-5] Some IMS-MS studies purposely modify the starting solvent composition (e.g. organic content, pH, temperature…) as a tentative to reach a large range of intracellular conditions and structural diversity.[1, 6-9] This approach provides additional insights into both stable and intermediate structures and allows to differentiate the solution structures retain in the gas-phase, known as memory effect, from the gas-phase structures.[10, 11] The same approach can be used in the gas-phase by changing the bath gas composition (e.g. N_2, N_2O, CO_2…)[12-14] or introducing bath gas modifiers (shift reagents)[15-17] in the ion mobility cell. Previous IMS-MS studies showed the utility of this approach to improve, in some cases, the separation between isomers.[4, 14, 17] This approach can be well-addressed using trapped ion mobility spectrometry (TIMS)[18, 19], which allows trapping ions in the gas-phase and exposing them to the bath gas modifiers at different trapping times (100-500 ms). Recent TIMS studies from our group showed the potential of bath gas modifiers to tailor the molecular environment of intrinsically disordered peptides (e.g., ATHP 3) and small proteins (e.g., heme proteins).[20, 21]

Relevant to the agonistic or antagonistic growth hormone – releasing hormone (GHRH) potencies, we recently proposed a high-throughput screening workflow based on structural motif descriptors using TIMS-MS for the elucidation of agonistic or antagonistic growth

hormone – releasing hormone (GHRH) potencies.[22] Briefly, GHRH is a hypothalamic neuropeptide

Table 1. Amino acid sequence of GHRH (1-29)-NH_2, MR-406 and MIA-602.

Peptides	Position of amino-acid residues															
	0	1	2	6	8	9	10	11	12	15	20	21	27	28	29	30
GHRH	H	Tyr	Ala	Phe	Asn	Ser	Tyr	Arg	Lys	Gly	Arg	Lys	Met	Ser	Arg	NH_2
MR-406	H	N-Me-Tyr	Ala	Phe	Gln	Ser	Tyr	Arg	Orn	Abu	Arg	Orn	Nle	Asp	Arg	NH-Me
MIA-602	PhAc-Ada	Tyr	D-Arg	Fpa_5	Ala	Har	N-Me-Tyr	His	Orn	Abu	His	Orn	Nle	D-Arg	Har	NH_2

Non-coded amino-acid residues and acyl groups used in the synthesis of the GHRH analogs are abbreviated as follows: Abu: α-aminobutyric acid; Ada: 12-aminododecanoic acid; Fpa_5: pentafluoro-phenylalanine; Har: homoarginine; Nle: norleucine; Orn: ornithine; PhAc: phenylacetyl.

comprising 44 residue (Figure S1a), where the activity resides in the N-terminal 1-29 residues (highlighted in green),[23] that stimulates the growth hormone secretion and release by binding to the GHRH receptor in the anterior pituitary gland.[24] Previous reports demonstrated the importance to synthesize GHRH agonists and antagonists due to their multiple therapeutic properties.[25-28] TIMS profiles exhibited different response to the solution molecular environment (native (10 mM ammonium acetate) vs. denaturing (50% methanol) conditions), inducing conformational changes reflected by the differences observed in the number and relative abundance of the IMS bands.[22] This clearly indicates a direct dependence on the molecular micro-environment in solution (i.e., starting solvent composition).

For a better description of the micro-environment effect on the conformational space of GHRH analogs, in the present work, we investigated the conformational states of GHRH (1-29), MR-406 (GHRH agonist, Figure S1b) and MIA-602 (GHRH antagonist, Figure S1c) (Table 1) as a function of the starting solvent methanol (MeOH), acetonitrile (MeCN) and acetone (Ac) composition as well as by introducing gas modifiers (e.g., MeOH, MeCN and Ac) in the bath gas of the TIMS analyzer (N_2). In the following discussion, a special emphasis is placed on the TIMS capability to follow the conformational states of GHRH analogs as a function of molecular micro-environment and trapping time (100-500 ms), providing additional insights on the structures and intermediates responsible for a given agonist or antagonist function.

2. EXPERIMENTAL SECTION

4.1. Materials and Reagents. GHRH (1-29) was purchased from Sigma Aldrich (St. Louis, MO). The GHRH agonist MR-406 and GHRH antagonist MIA-602 were provided by A.V. Schally group.[29, 30] Briefly, GHRH analogs were obtained using solid-phase method and purified by reversed-phase HPLC as previously reported.[29-31] MeOH, MeCN, Ac and ammonium acetate (NH_4Ac) were purchased from Fisher Scientific (Pittsburgh, PA). GHRH analogs were dissolved to 5 μM in 10 mM aqueous NH_4Ac for native conditions, and in 50:50 (v/v) H_2O/MeOH, H_2O/MeCN and H_2O/Ac for denaturing conditions. Low-concentration Tuning Mix (G1969-85000) was used to calibrate the instrument and obtained from Agilent Technologies (Santa Clara, CA).

4.2. TIMS-MS Experiments. A custom built nanoESI-TIMS coupled to an Impact Q-TOF mass spectrometer (Bruker, Billerica, MA, Figure S2) was employed to perform the ion mobility experiments.[18] A custom software in LabView (National Instruments) was used to control the TIMS unit and synchronized with the MS platform controls.[19] Briefly, TIMS is based on holding the ions stationary using an electric field (E) against a moving buffer gas.[18] In TIMS operation, a radio frequency (rf) voltage is applied to the electrodes of the TIMS analyzer to generate a radially confining pseudopotential and an axial electric field gradient is produced across the electrodes to counteract the drag force exerted by the gas flow to trap the ions in the TIMS analyzer. Ions are eluted from the TIMS analyzer region by decreasing the axial electric field (Figure S2). TIMS separation depends on the gas flow velocity (v_g), elution voltage ($V_{elution}$), ramp time (t_{ramp}) and base voltage (V_{out}).[18, 19] The reduced mobility, K_o, is defined by:

$$K_0 = \frac{v_g}{E} \cong \frac{A}{(V_{elution} - V_{out})} \quad (1)$$

The constant *A* was determined using known reduced mobilities of Tuning Mix component.[32] Solvents were introduced in peptide solutions prior to TIMS-MS analysis. Peptide sample solutions were loaded in a pulled-tip capillary and directly infused into the MS inlet and sprayed at 700-1200 V. Gas-phase modifiers were added to the TIMS cell by nebulization (Figure S2) at atmospheric pressure using a second inlet at 650 mL/min (Analyt-MTC, Müllheim, Germany) defined by the system geometry impedance. TIMS-MS experiments were performed using nitrogen (N_2) as well as N_2+MeOH, N_2+MeCN and N_2+Ac at room temperature. The gas velocity was kept constant between the funnel entrance ($P1$ = 2.6 mbar) and exit ($P2$ = 1.1 mbar, Figure S2) regardless of the bath gas composition. An rf voltage of 250 V_{pp} at 880 kHz was applied to all electrodes. TIMS experiments were performed using a voltage ramp (V_{ramp}) of -280 to 0 V and base voltage (V_{out}) of 60 V. TIMS spectra were collected for t_{ramp} = 100 - 500 ms. It should be noted that all solution molecular micro-environment studies were performed with N_2 as the bath gas, and that all gas-phase molecular micro-environment were conducted using 10 mM aqueous NH4AC starting solvent composition.

3. RESULTS AND DISCUSSION

The high mobility resolution and trapping nature of TIMS-MS has permitted the study of kinetically trapped intermediates of biomolecules in their native and non-native states providing the distribution of conformational states and their dependence on the molecular micro-environment.[33-35] The composition of the starting solvent[36, 37] and bath gas[20, 21] conditions can induce conformational changes reflected in the charge state distribution as well as in the number of mobility bands. The mass spectrometry analysis of the investigated GHRH analogs in native conditions resulted in a charge state distribution of $[M+3H]^{3+}$ to $[M+4H]^{4+}$ for GHRH (1-29) (Figure 1a, yellow panel) and MR-406 (Figure 2a, yellow panel) and $[M+3H]^{3+}$ to $[M+6H]^{6+}$ for MIA-602 (Figure 3a, yellow panel). Main changes in the charge state distribution arise from differences in the number of basic residues present in the sequence of GHRH analogs. In fact, GHRH (1-29) and MR-406 have five basic residues (position 11, 12, 20, 21 and 29, Figures S1a and S1b) while MIA-602 has eight basic residues (position 2, 9, 11, 12, 20, 21, 28 and 29, Figure S1c). The charge state distribution of the investigated GHRH analogs exhibited a dependence on the solution molecular micro-environment (i.e., starting solvent composition, Figure 1a-3a, red panel). As a general trend, an increase in the relative abundance of the higher charge states was observed when incorporating organic content in the starting solvent composition due to molecular rearrangements causing the exposure of basic residues. For example, an increase in the relative abundance of the $[M+5H]^{5+}$ and $[M+6H]^{6+}$ species was observed for MIA-

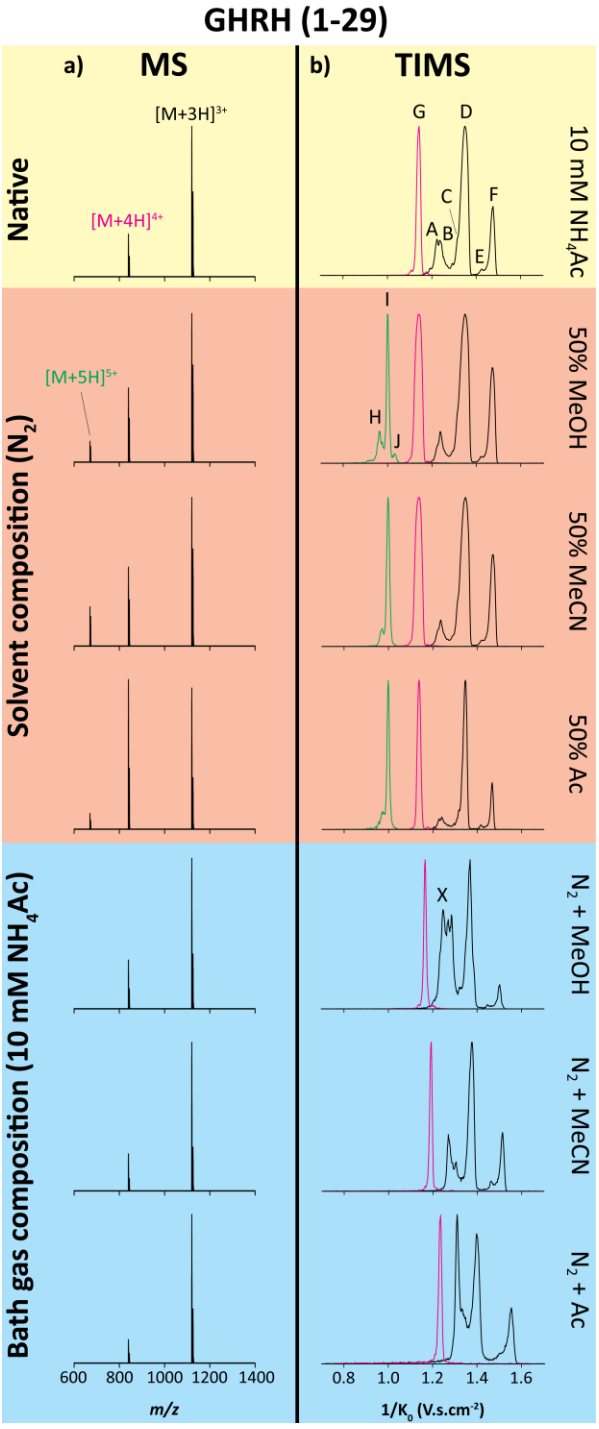

Figure 1. Mass (a) and ion mobility (b) spectra of GHRH (1-29) as a function of the starting solvent composition (yellow and red panels) and bath gas composition (blue panel). The $[M+3H]^{3+}$, $[M+4H]^{4+}$ and $[M+5H]^{5+}$ species are represented

by black, magenta and green traces, respectively. Note that within each charge state, increasing $1/K_o$ leads to higher collision cross sections (CCS). Moreover, CCS increases with the charge state.

602 upon the addition of organic matter in the starting solvent composition (Figure 3a, red panel). In addition, the presence of organic content in the starting solvent composition showed a conformational change in the GHRH (1-29) (Figure 1a, red panel) and MR-406 (Figure 2a, red panel) reflected by the presence of an additional charge state ($[M+5H]^{5+}$). As expected, changes in the bath gas composition (neutral molecules) did not affected the MS distribution, suggesting that the MS profile is just a reflection of the charge state distribution during native conditions and charge transfer reactions do not occurred in the IMS cell (Figure 1a-3a, blue panel).

The ion mobility analysis of the GHRH analogs resulted in multiple conformational states (i.e., IMS bands) for most of the charge states in native conditions (Figure 1b-3b, yellow panel). The large diversity of IMS bands, especially for the lower charge states, could be explained by the presence of conformers resulting from the flexibility of the GHRH analogs and/or the presence of numerous basic residues that involves a competition for the protonation site. Under native solvent conditions (i.e., 10 mM NH_4Ac), GHRH (1-29) and MR-406 exhibited six (A-F, Figure 1b, yellow panel) and seven (a-g, Figure 2b, yellow panel) conformers for the $[M+3H]^{3+}$ species (black traces), respectively, while a unique IMS band was obtained for the $[M+4H]^{4+}$ species of GHRH (1-29) (G) and MR-406 (h) (magenta traces). For MIA-602, TIMS-MS experiments identified six (1-6, Figure 3b, yellow panel) conformers for the $[M+3H]^{3+}$ species (black trace), four (7-10) for the $[M+4H]^{4+}$ species (magenta traces), one (11) for the $[M+5H]^{5+}$ species (green traces) and three (12-14) IMS bands for the $[M+6H]^{6+}$ species (purple traces).

The number of mobility bands were conserved across the different organic solvent compositions (Figure 1b-3b, red panel); however, significant changes in the relative abundance of the conformational states of GHRH analogs were observed according to the organic solvent composition. For example, a decrease in the relative abundance of the most compact structures of the $[M+3H]^{3+}$ species (black traces) of GHRH (1-29) (IMS bands A and B, Figure 1b, red panel) and MR-406 (IMS bands a-c, Figure 2b, red panel) was observed in the presence of methanol combined with an increase of the most extended conformer of the $[M+3H]^{3+}$ species for GHRH (1-29) (IMS band F) and MR-406 (IMS band g). For MIA-602, this feature was less pronounced but a slight increase in the relative abundance was observed for the most compact structure of the $[M+6H]^{6+}$ species (IMS band 12, Figure 3b, red panel, purple traces). In the presence of acetonitrile, the features observed for the $[M+3H]^{3+}$ species was less pronounced as compared to methanol but a substantial increase of the relative abundance of the IMS band 12 was obtained for MIA-602. Drastic changes were observed in the presence of acetone

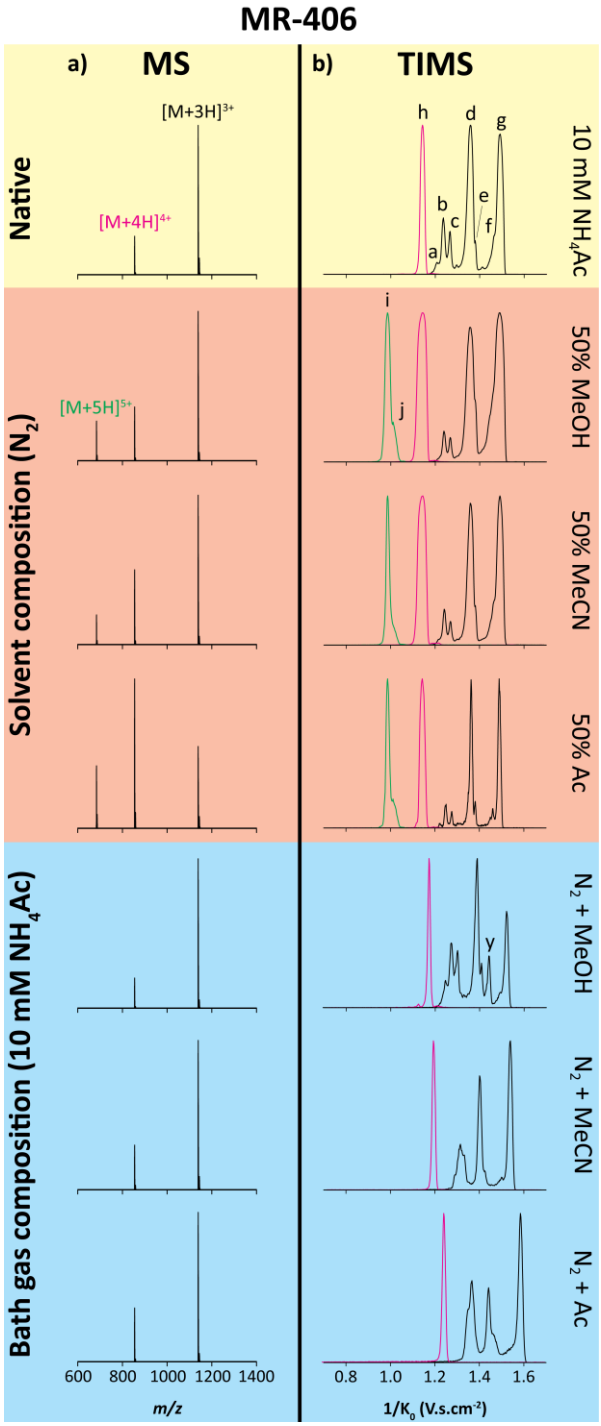

Figure 2. Mass (a) and ion mobility (b) spectra of MR-406 as a function of the starting solvent composition (yellow and red panels) and bath gas composition (blue panel). The $[M+3H]^{3+}$, $[M+4H]^{4+}$ and $[M+5H]^{5+}$ species are represented

by black, magenta and green traces, respectively. Note that within each charge state, increasing $1/K_o$ leads to higher collision cross sections (CCS). Moreover, CCS increases with the charge state.

especially for MIA-602 as reflected by the TIMS profiles of the $[M+3H]^{3+}$ and $[M+4H]^{4+}$ species (Figure 3b, red panel, black and magenta traces). Changes in the TIMS profiles showed the dependence of the conformational states of GHRH analogs according to the molecular environment in solution, suggesting the presence of memory effects from the solution structures retain in the gas-phase. The changes in the conformational states can be explained by different type of intermolecular interactions (e.g., salt bridges and hydrogen bonds) with a specific functional group. For example, the carbonyl group of acetone can form additional hydrogen bonds with the amide group of the peptide, reflected by more compact structures in the TIMS profiles as compared to methanol or acetonitrile that probably disrupt some of the hydrogen bonds as reflected by an increase in the relative abundance of the most extended structures. Another explanation could be for the GHRH analogs to adopt different charge solvation schemes according to the molecular environment, possibly including salt bridges. These suggestion are in good agreement with previous observations of structural rearrangements.[1, 3, 11, 20, 21]

The ion mobility analysis of the GHRH analogs exhibited significant changes in the TIMS profiles with the bath gas composition when compared to the solution studies (Figure 1b-3b, blue panel). The use of gas modifiers resulted in mobility shifts toward smaller mobilities across the GHRH analogs that are correlated with the size and mass of the organic modifiers, methanol (32 Da), acetonitrile (41 Da) and acetone (58 Da). In fact, methanol as a gas modifier causes the smallest increase in $1/K_o$ while acetone induces the largest increase (Figure 1b-3b, blue panel). Despite of the changes in $1/K_o$, most of the mobility bands were found conserved for all the charge states across the different bath gas compositions (Figure 1b-3b, blue panel). However, changes in the relative abundance of the IMS bands of GHRH analogs were observed with the bath gas composition, different from the previous trend observed with the solution composition. For example, a significant decrease in the relative abundance of the most extended structure of the $[M+3H]^{3+}$ species (black traces) of GHRH (1-29) (IMS band F, Figure 1b, blue panel), MR-406 (IMS band g, Figure 2b, blue panel) and MIA-602 (IMS band 6, Figure 3b, blue panel) was observed in the presence of methanol gas modifier combined with an increase of the most compact conformers for the $[M+3H]^{3+}$ species of GHRH (1-29) (IMS bands A and B), MR-406 (IMS bands a-c) and MIA-602 (IMS bands 1-5). The same feature was observed for the $[M+4H]^{4+}$ (magenta traces) and $[M+6H]^{6+}$ (purple traces) species of MIA-602 (Figure 3b). Similar trends were also observed for GHRH (1-29) (Figure 1b, blue panel) and MIA-602 (Figure 3b, blue panel) in the

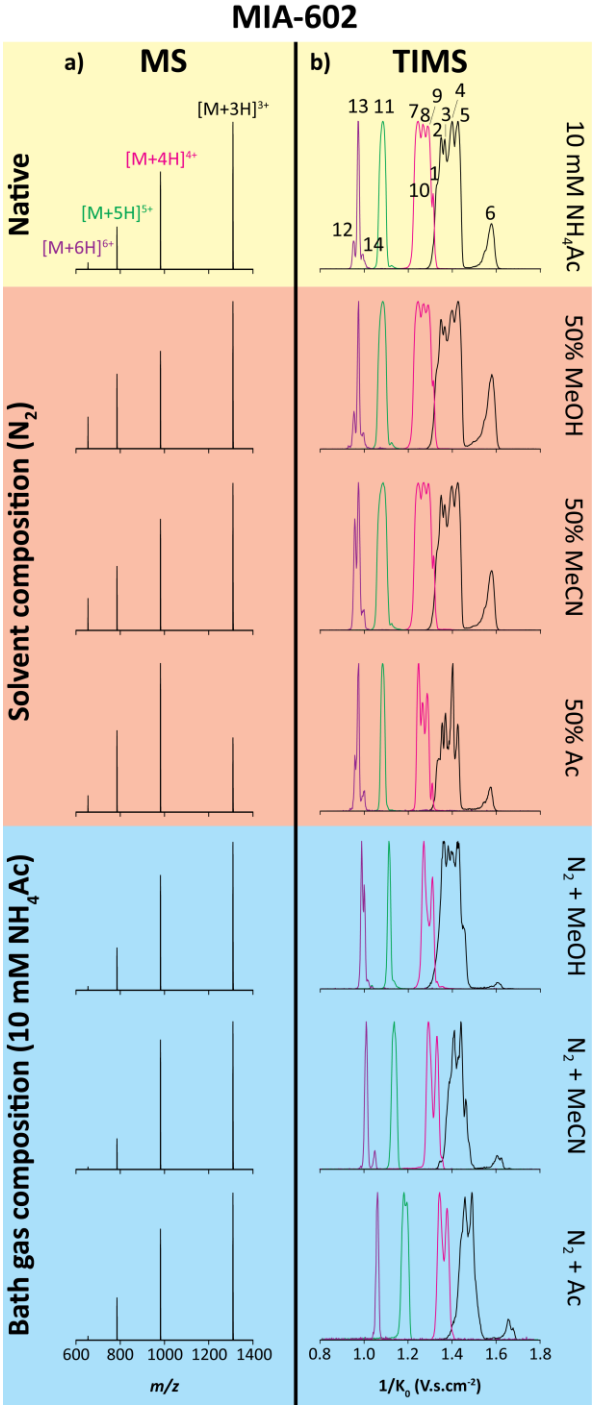

Figure 3. Mass (a) and ion mobility (b) spectra of MIA-602 as a function of the starting solvent composition (yellow and red panels) and bath gas composition (blue panel). The $[M+3H]^{3+}$, $[M+4H]^{4+}$, $[M+5H]^{5+}$ and $[M+6H]^{6+}$ species are

represented by black, magenta, green and purple traces, respectively. Note that within each charge state, increasing $1/K_0$ leads to higher collision cross sections (CCS). Moreover, CCS increases with the charge state.

presence of acetonitrile or acetone in the TIMS cell. The presence of acetonitrile or acetone in the TIMS cell had different effects on the conformational structures of MR-406 (Figure 2b, blue panel), where an increase in the relative abundance of the most compact (IMS bands a-c) and extended (IMS band g) structures for the $[M+3H]^{3+}$ species (black trace) is observed combined with a substantial decrease of the IMS band d that was not obtained in methanol as gas modifier. Moreover, an additional IMS band was observed in the case of the $[M+3H]^{3+}$ species (black traces) of GHRH (1-29) (IMS band X, Figure 1b, blue panel) and MR-406 (IMS band y, Figure 2b, blue panel). These IMS bands can be interpreted by the effect of the gas modifier on the peptide environment that shift the IMS bands X and y for which it was not separated with the native conditions and probably overlaid with another IMS band.

In general, TIMS profiles showed a dependence of the conformational states of GHRH analogs with the molecular micro-environment in the gas-phase different from those induced in solution. The changes in the conformational states of GHRH analogs in the presence of gas-phase modifiers can be driven by a clustering/de-clustering mechanism between the peptides and the gas modifier, while trapped in the TIMS cell as previously described.[21] This involves different type of intermolecular interactions as observed in solution, including ion-dipole and/or dipole-dipole interactions between the gas modifier and the basic and/or polar residues thus allows a change in the energy landscape favoring a new equilibrium across conformers. The dipole moments of the investigated gas modifiers have similar (MeOH) or higher (MeCN and Ac) values than that of water favoring clustering in the gas-phase and are consistent with the different TIMS profiles obtained using methanol as compared to acetonitrile or acetone gas modifier (Figure 1b-3b, blue panel).

The ion mobility analysis of the GHRH analogs also exhibited changes in the TIMS profiles as a function of the trapping time inducing structural rearrangements toward the more stable and energetically favoured structures (Figures 4 and S3-S6). It should be noted that the kinetic experiments are only presented for the $[M+3H]^{3+}$ (Figure 4) species of the GHRH analogs as well as the $[M+4H]^{4+}$ (Figure 4) and $[M+6H]^{6+}$ (Figure S6) species of MIA-602, for which multiple IMS bands are observed through all the solvent and gas modifier conditions. A common trend was observed for the $[M+3H]^{3+}$ species of GHRH (1-29) when varying the solvent composition, where the relative abundance of the most intense conformer (IMS band D, Figure 4, yellow/red panels, magenta traces) is increasing with the trapping time while the other IMS bands were slightly decreased or constant, involving that the IMS band D is the most stable structure in the gas-phase. The same trend was also obtained in the presence of methanol in the TIMS cell. However, when introducing acetonitrile and acetone in the TIMS cell, which have significantly higher dipole moment as compared to methanol and water, a decrease in the relative abundance of the IMS band D and the most extended structures (IMS bands C, E and F) is obtained combined with an increase of the most compact structures (IMS bands X, A and B) that become the most energetically favored conformers (Figure 4, blue panel). In fact, MeCN and Ac have the potential to form stronger ionic interactions with the amino acid residues than water or MeOH due to higher polarity. Then the observed differences in TIMS profiles of GHRH (1-29) toward more compact structures upon exposition to MeCN and Ac could be originated by the presence of additional inter- and/or intramolecular interactions, which are more pronounced by increasing exposition (trapping time) to MeCN and Ac, that allow for changes in the energy landscape of the peptide favoring a new equilibrium across conformers.

In the case of the $[M+3H]^{3+}$ species of MR-406, a common trend was observed between native and methanol and acetonitrile solvent composition, where the relative abundance of the two most intense conformer (IMS bands d and g, Figure 4, yellow/red panels, magenta/purple traces) is increasing with the trapping time with a more pronounced effect for the IMS band g which is the most stable gas-phase structure in native, methanol and acetonitrile solution. However, a conformational interconversion was observed between the IMS bands d and g in the presence of acetone solution involving that the IMS band d is the most stable gas-phase structure in acetone solution. In the presence of methanol in the TIMS cell, an increase in the relative abundance of the IMS band d was observed combined with a decrease of a more compact structure (IMS band b). In addition, as observed in the case of GHRH (1-29) when introducing acetonitrile and acetone in the TIMS cell, a significant decrease in the relative abundance of the most extended structures (IMS bands d, f and g) is obtained combined with an increase of the most compact structures (IMS bands a-c) that become the most energetically favored conformers (Figure 4, blue panel).

In the case of the $[M+3H]^{3+}$ species of MIA-602, a common trend was observed between all the starting solvent composition, where the relative abundance of the IMS bands 2 and 5 are increasing with the trapping time while the IMS bands 1 and 6 are decreasing, involving that the IMS bands 2 and 5 are the most stable structures in

the gas-phase (Figure 4, yellow/red panels). No conformational changes were observed in the presence of gas modifiers except for a conformational interconversion between the IMS bands 2 and 5 (Figure

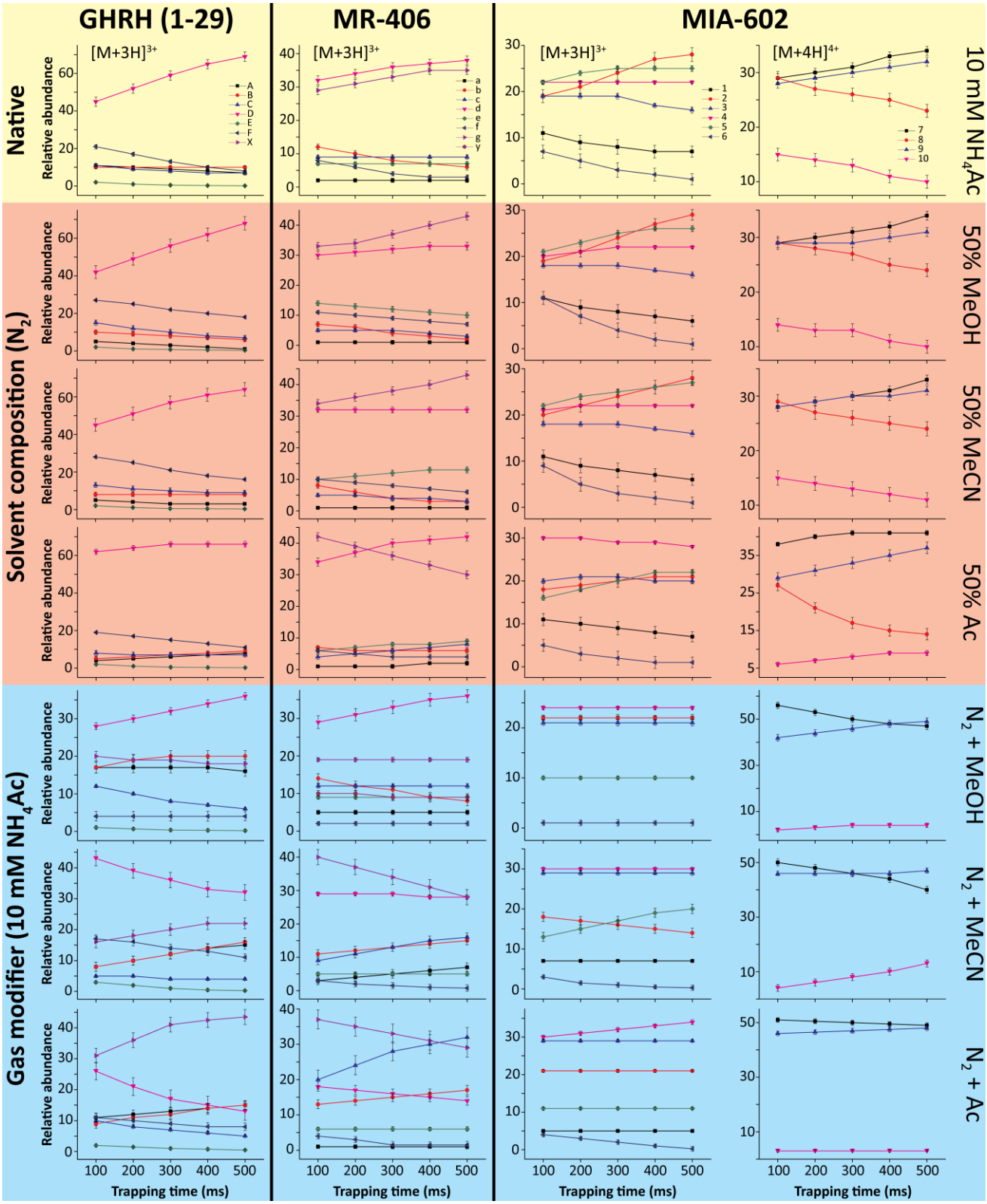

Figure 4. Kinetic plots for the multiply protonated species of GHRH (1-29), MR-406 and MIA-602 representing the relative abundance of the IMS bands as a function of the trapping time are shown for the starting solvent composition (yellow and red panels) and bath gas composition (blue panel). Error bars are illustrated by black lines.

4, blue panel). For the $[M+4H]^{4+}$ species, the IMS bands 7 and 9 were increoasing through all the starting solvent composition while the IMS bands 8 and 10 tended to decrease (yellow/red panels). While the relative abundance of the IMS band 9 was still increased in the presence of a bath gas modifier, the IMS band 7 are now decreasing making the structure of the IMS band 9 the most stable in the gas-phase. Finally, the $[M+6H]^{6+}$ species showed a conformational interconversion between the IMS bands 12 and 13, where the most compact structure (IMS band 12) is the more stable conformer (Figure S6). The present methodology implemented additional insights on the intermediates and the most stables structures that are probably driving the agonist and antagonist activities of GHRH analogs.

3. CONCLUSIONS

This study showcases the impact of the starting solvent and bath gas compositions on the conformational states of three GHRH analogs, ranging from agonist to wild type to antagonist. The present results revealed that the number of IMS bands were preserved in both solution and gas-phase molecular micro-environment, but with a dependence on the relative abundance. Memory effects from the solution structures were observed in the gas-phase structures. The changes in the TIMS profiles induced by the use of dopants in the gas-phase molecular micro-environment were different from the changes observed using solution additives. We interpret these differences as a clustering and de-clustering mechanisms between the molecular GHRH analog ions and the neutral bath gas modifiers, driven by changes in the free energy landscape and interconversion barriers between conformers due to higher order ion-neutral interactions (e.g., ion-dipole and/or dipole-dipole interactions). Moreover, conformational interconversions were observed as a function of the trapping time (100-500 ms) toward the more stable "gas-phase" structures. TIMS experiments as a function of both solvent and bath gas composition and trapping time enabled us to outline a more detailed description of the multiple intermediates of GHRH analogs and potential links to the agonist and antagonist activity GHRH (1-29), MR-406 and MIA-602.

ASSOCIATED CONTENT

Supporting Information

Additional Figures illustrating the amino acid sequence of the GHRH (1-44), MR-406 and MIA-602, TIMS-MS instrument showing the TIMS cell schematic and TIMS operation, ion mobility profiles of GHRH analogs as a function of the trapping time and kinetic plots for the $[M+6H]^{6+}$ of MIA-602. This material is available free of charge via the Internet at http://pubs.acs.org.

AUTHOR INFORMATION

Corresponding Author

* Email: fernandf@fiu.edu

Author Contributions

KJDF and JM contributed equally to this work. The manuscript was written through contributions of all authors. All authors have given approval to the final version of the manuscript.

Notes

The authors declare no competing financial interest.

ACKNOWLEDGEMENTS

The authors acknowledge the financial support from the National Science Foundation Division of Chemistry, under CAREER award CHE-1654274, with co-funding from the Division of Molecular and Cellular Biosciences to FFL. We thank A.V. Schally group for providing the GHRH analogs.

REFERENCES

1. El-Baba, T. J.; Fuller, D. R.; Hales, D. A.; Russell, D. H.; Clemmer, D. E. Solvent Mediation of Peptide Conformations: Polyproline Structures in Water, Methanol, Ethanol, and 1-Propanol as Determined by Ion Mobility Spectrometry-Mass Spectrometry. *J. Am. Soc. Mass Spectrom.* **2019**, *30*, 77-84.
2. Lanucara, F.; Holman, S. W.; Gray, C. J.; Eyers, C. E. The Power of Ion Mobility-Mass Spectrometry for Structural Characterization and the Study of Conformational Dynamics. *Nat. Chem.* **2014,** *6*, 281-294.
3. Ruotolo, B. T.; Russell, D. H. Gas-Phase Conformations of Proteolytically Derived Protein Fragments: Influence of Solvent on Peptide Conformation. *J. Phys. Chem. B.* **2004,** *108*, 15321-15331.
4. Dwivedi, P.; Wu, C.; Matz, L. M.; Clowers, B. H.; Siems, W. F.; Hill, H. H., Jr. Gas-Phase Chiral Separations by Ion Mobility Spectrometry. *Anal. Chem.* **2006,** *78*, 8200-8206.
5. Bush, M. F.; Campuzano, I. D.; Robinson, C. V. Ion Mobility Mass Spectrometry of Peptide Ions: Effects of Drift Gas and Calibration Strategies. *Anal. Chem.* **2012,** *84*, 7124-7130.
6. Li, J.; Taraszka, J. A.; Counterman, A. E.; Clemmer, D. E. Influence of Solvent Composition and Capillary Temperature on the Conformations of Electrosprayed Ions: Unfolding of Compact Ubiquitin Conformers from Pseudonative and Denatured Solutions. *Int. J. Mass Spectrom.* **1999,** *185-187*, 37-47.
7. Butcher, D.; Bernad, S.; Derrien, V.; Sebban, P.; Miksovska, J.; Fernandez-Lima, F. Non-Symbiotic Hemoglobin Conformational Space Dependence on the Heme Coordination

using nESI-TIMS-TOF MS. *Int. J. Mass Spectrom.* **2018,** *430*, 37-43.

8. Vahidi, S.; Stocks, B. B.; Konermann, L. Partially Disordered Proteins Studied by Ion Mobility-Mass Spectrometry: Implications for the Preservation of Solution Phase Structure in the Gas Phase. *Anal. Chem.* **2013,** *85*, 10471-10478.

9. Valentine, S. J.; Clemmer, D. E. Temperature-Dependent H/D Exchange of Compact and Elongated Cytochrome c Ions in the Gas Phase. *J. Am. Soc. Mass Spectrom.* **2002,** *13*, 506-517.

10. Wyttenbach, T.; Bowers, M. T. Structural Stability from Solution to the Gas Phase: Native Solution Structure of Ubiquitin Survives Analysis in a Solvent-Free Ion Mobility-Mass Spectrometry environment. *J. Phys. Chem. B.* **2011,** *115*, 12266-12275.

11. Pierson, N. A.; Chen, L.; Valentine, S. J.; Russell, D. H.; Clemmer, D. E. Number of Solution States of Bradykinin from Ion Mobility and Mass Spectrometry Measurements. *J. Am. Chem. Soc.* **2011,** *133*, 13810-13813.

12. Kanu, A. B.; Hill, H. H., Jr. Identity Confirmation of Drugs and Explosives in Ion Mobility Spectrometry using a Secondary Drift Gas. *Talanta* **2007,** *73*, 692-699.

13. Lalli, P. M.; Corilo, Y. E.; Fasciotti, M.; Riccio, M. F.; de Sa, G. F.; Daroda, R. J.; Souza, G. H.; McCullagh, M.; Bartberger, M. D.; Eberlin, M. N.; *et al*. Baseline Resolution of Isomers by Traveling Wave Ion Mobility Mass Spectrometry: Investigating the Effects of Polarizable Drift Gases and Ionic Charge Distribution. *J. Mass Spectrom.* **2013,** *48*, 989-997.

14. Poyer, S.; Loutelier-Bourhis, C.; Tognetti, V.; Joubert, L.; Enche, J.; Bossée, A.; Mondeguer, F.; Hess, P.; Afonso, C. Differentiation of Gonyautoxins by Ion Mobility–Mass Spectrometry: A Cationization Study. *Int. J. Mass Spectrom.* **2016,** *402*, 20-28.

15. Howdle, M. D.; Eckers, C.; Laures, A. M.; Creaser, C. S. The Use of Shift Reagents in Ion Mobility-Mass Spectrometry: Studies on the Complexation of an Active Pharmaceutical Ingredient with Polyethylene Glycol Excipients. *J. Am. Soc. Mass Spectrom.* **2009,** *20*, 1-9.

16. Hilderbrand, A. E.; Myung, S.; Clemmer, D. E. Exploring Crown Ethers as Shift Reagents for Ion Mobility Spectrometry. *Anal. Chem.* **2006,** *78*, 6792-6800.

17. Fernandez-Maestre, R.; Wu, C.; H. Hill, H. Nitrobenzene as a Buffer Gas Modifier in Ion Mobility Spectrometry: Better Separations and Cleaner Spectra. *Curr. Anal. Chem.* **2013,** *9*, 485-494.

18. Fernandez-Lima, F.; Kaplan, D. A.; Suetering, J.; Park, M. A. Gas-Phase Separation using a Trapped Ion Mobility Spectrometer. *Int. J. Ion Mobil. Spectrom.* **2011,** *14*, 93-98.

19. Fernandez-Lima, F. A.; Kaplan, D. A.; Park, M. A. Note: Integration of Trapped Ion Mobility Spectrometry with Mass Spectrometry. *Rev. Sci. Instrum.* **2011,** *82*, 126106.

20. Garabedian, A.; Leng, F. F.; Ridgeway, M. E.; Park, M. A.; Fernandez-Lima, F. Tailoring Peptide Conformational Space with Organic Gas Modifiers in TIMS-MS. *Int. J. Ion Mobil. Spectrom.* **2018,** *21*, 43-48.

21. Butcher, D.; Miksovska, J.; Ridgeway, M. E.; Park, M. A.; Fernandez-Lima, F. The Effects of Solution Additives and Gas-Phase Modifiers on the Molecular Environment and Conformational Space of Common Heme Proteins. *Rapid Commun. Mass Spectrom.* **2019**, *33*, 399-404.

22. Jeanne Dit Fouque, K.; Salgueiro, L. M.; Cai, R.; Sha, W.; Schally, A. V.; Fernandez-Lima, F. Structural Motif Descriptors as a Way To Elucidate the Agonistic or Antagonistic Activity of Growth Hormone–Releasing Hormone Peptide Analogues. *ACS Omega* **2018,** *3*, 7432-7440.

23. Vance, M. L. Growth-Hormone-Releasing Hormone. *Clin. Chem.* **1990,** *36*, 415-420.

24. Schally, A. V.; Varga, J. L.; Engel, J. B. Antagonists of Growth-Hormone-Releasing Hormone: an Emerging New Therapy for Cancer. *Nat. Clin. Pract. Endocrinol. Metab.* **2008,** *4*, 33-43.

25. Schally, A. V. New Approaches to the Therapy of Various Tumors Based on Peptide Analogues. *Horm. Metab. Res.* **2008,** *40*, 315-322.

26. Letsch, M.; Schally, A. V.; Busto, R.; Bajo, A. M.; Varga, J. L. Growth Hormone-Releasing Hormone (GHRH) Antagonists Inhibit the Proliferation of Androgen-Dependent and -Independent Prostate Cancers. *Proc. Natl. Acad. Sci. USA.* **2003,** *100*, 1250-1255.

27. Ludwig, B.; Ziegler, C. G.; Schally, A. V.; Richter, C.; Steffen, A.; Jabs, N.; Funk, R. H.; Brendel, M. D.; Block, N. L.; Ehrhart-Bornstein, M.; *et al*. Agonist of Growth Hormone-Releasing Hormone as a Potential Effector for Survival and Proliferation of Pancreatic Islets. *Proc. Natl. Acad. Sci. USA.* **2010,** *107*, 12623-12628.

28. Kanashiro-Takeuchi, R. M.; Tziomalos, K.; Takeuchi, L. M.; Treuer, A. V.; Lamirault, G.; Dulce, R.; Hurtado, M.; Song, Y.; Block, N. L.; Rick, F.; *et al*. Cardioprotective Effects of Growth Hormone-Releasing Hormone Agonist After Myocardial Infarction. *Proc. Natl. Acad. Sci. USA.* **2010,** *107*, 2604-2609.

29. Zarandi, M.; Cai, R.; Kovacs, M.; Popovics, P.; Szalontay, L.; Cui, T.; Sha, W.; Jaszberenyi, M.; Varga, J.; Zhang, X.; *et al*. Synthesis and Structure-Activity Studies on Novel Analogs of Human Growth Hormone Releasing Hormone (GHRH) with Enhanced Inhibitory Activities on Tumor Growth. *Peptides* **2017,** *89*, 60-70.

30. Cai, R.; Schally, A. V.; Cui, T.; Szalontay, L.; Halmos, G.; Sha, W.; Kovacs, M.; Jaszberenyi, M.; He, J.; Rick, F. G.; *et al*. Synthesis of New Potent Agonistic Analogs of Growth Hormone-Releasing Hormone (GHRH) and Evaluation of their Endocrine and Cardiac Activities. *Peptides* **2014,** *52*, 104-112.

31. Zarandi, M.; Horvath, J. E.; Halmos, G.; Pinski, J.; Nagy, A.; Groot, K.; Rekasi, Z.; Schally, A. V. Synthesis and Biological Activities of Highly Potent Antagonists of Growth Hormone-Releasing Hormone. *Proc. Natl. Acad. Sci. USA.* **1994,** *91*, 12298-12302.

32. Hernandez, D. R.; Debord, J. D.; Ridgeway, M. E.; Kaplan, D. A.; Park, M. A.; Fernandez-Lima, F. Ion Dynamics in a Trapped Ion Mobility Spectrometer. *Analyst* **2014,** *139*, 1913-1921.

33. Schenk, E. R.; Almeida, R.; Miksovska, J.; Ridgeway, M. E.; Park, M. A.; Fernandez-Lima, F. Kinetic Intermediates of Holo- and Apo-Myoglobin Studied Using HDX-TIMS-MS and Molecular Dynamic Simulations. *J. Am. Soc. Mass Spectrom.* **2015,** *26*, 555-563.

34. Molano-Arevalo, J. C.; Hernandez, D. R.; Gonzalez, W. G.; Miksovska, J.; Ridgeway, M. E.; Park, M. A.; Fernandez-Lima, F. Flavin Adenine Dinucleotide Structural Motifs: from Solution to Gas Phase. *Anal. Chem.* **2014,** *86*, 10223-10230.

35. Garabedian, A.; Butcher, D.; Lippens, J. L.; Miksovska, J.; Chapagain, P. P.; Fabris, D.; Ridgeway, M. E.; Park, M. A.;

Fernandez-Lima, F. Structures of the Kinetically Trapped i-Motif DNA Intermediates. *Phys. Chem. Chem. Phys.* **2016,** *18*, 26691-26702.

36. Molano-Arevalo, J. C.; Jeanne Dit Fouque, K.; Pham, K.; Miksovska, J.; Ridgeway, M. E.; Park, M. A.; Fernandez-Lima, F. Characterization of Intramolecular Interactions of Cytochrome c Using Hydrogen-Deuterium Exchange-Trapped Ion Mobility Spectrometry-Mass Spectrometry and Molecular Dynamics. *Anal. Chem.* **2017,** *89*, 8757-8765.

37. Molano-Arevalo, J. C.; Gonzalez, W.; Jeanne Dit Fouque, K.; Miksovska, J.; Maitre, P.; Fernandez-Lima, F. Insights from Ion Mobility-Mass Spectrometry, Infrared Spectroscopy, and Molecular Dynamics Simulations on Nicotinamide Adenine Dinucleotide Structural Dynamics: NAD(+) vs. NADH. *Phys. Chem. Chem. Phys.* **2018,** *20*, 7043-7052.

TOC Graphic